Repeated TLR9 stimulation results in macrophage activation syndrome–like disease in mice

Edward M. Behrens,[1] Scott W. Canna,[1] Katharine Slade,[1] Sheila Rao,[2] Portia A. Kreiger,[3] Michele Paessler,[4] Taku Kambayashi,[5] and Gary A. Koretzky[6,7]

[1]Division of Rheumatology, The Children's Hospital of Philadelphia, Philadelphia, Pennsylvania, USA. [2]Immunology Graduate Group, University of Pennsylvania, Philadelphia, Pennsylvania, USA. [3]Department of Pathology, Alfred I. duPont Hospital for Children, Wilmington, Delaware, USA. [4]Department of Pathology, The Children's Hospital of Philadelphia, Philadelphia, Pennsylvania, USA. [5]Department of Pathology, [6]Department of Medicine, and [7]Abramson Family Cancer Research Institute, University of Pennsylvania, Philadelphia, Pennsylvania, USA.

Hemophagocytic lymphohistiocytosis (HLH) and macrophage activation syndrome (MAS) are 2 similar diseases characterized by a cytokine storm, overwhelming inflammation, multiorgan dysfunction, and death. Animal models of HLH suggest that disease is driven by IFN-γ produced by $CD8^+$ lymphocytes stimulated by persistent antigen exposure. In these models and patients with "primary" HLH, the antigen persists due to genetic defects, resulting in ineffective cytotoxic responses by $CD8^+$ T cells and poor pathogen clearance. However, infectious triggers are often not identified in patients with MAS, and some patients with HLH or MAS lack defects in cytotoxic T cell killing. Herein, we show that repeated stimulation of TLR9 produced an HLH/MAS-like syndrome on a normal genetic background, without exogenous antigen. Like previous HLH models, TLR9-induced MAS was IFN-γ dependent; however, unlike other models, disease did not require lymphocytes. We further showed that IL-10 played a protective role in this model and that blocking IL-10 signaling led to the development of hemophagocytosis. IL-10 may therefore be an important target for the development of effective therapeutics for MAS. Our data provide insight into MAS-like syndromes in patients with inflammatory diseases in which there is chronic innate immune activation but no genetic defects in cytotoxic cell function.

Introduction

Sepsis, hemophagocytic lymphohistiocytosis (HLH), macrophage activation syndrome (MAS), and systemic inflammatory response syndrome (SIRS, e.g., sepsis without a documented pathogen) are different clinical entities that likely represent a common immunopathologic state referred to as cytokine storm (1). The designation given any particular patient's cytokine storm syndrome is generally determined by whether an underlying trigger can be found: bacterial infection (2), malignancy or genetic defect (3), rheumatologic disease (4), or idiopathic or drug induced (1), respectively. Despite the different names, these syndromes share more in common than not (5): massive inflammatory response, elevated serum cytokine levels, multiorgan system disease, hemophagocytic macrophages, and often death. These syndromes are often clinically indistinguishable (5). However, the cytokines that predominate in each of these syndromes may differ; for instance, TNF-α predominates in bacterial sepsis (6), and IFN-γ predominates in HLH and MAS (7, 8). What drives the systemic toxicity in these diseases is not clear. Much attention has recently been given to primary HLH due to our increased understanding of the genetic defects involved. Primary HLH is caused by genetic defects in cytotoxic granule exocytosis, such that $CD8^+$ T cells are unable to kill virally infected targets. The current model proposes that overstimulation of adaptive immunity leads to the progression of disease. This occurs via continuous antigen stimulation from infected antigen-presenting cells to $CD8^+$ T cells, resulting in the production of IFN-γ that directly leads to toxicity, a cycle that is not terminated because the $CD8^+$ T cells are unable to lyse their target cells (8). However, attempting to recapitulate HLH by continuous antigen exposure does not completely recreate the disease process, suggesting that persistent antigenemia is not sufficient (8). In the case of MAS and SIRS, defects in cytotoxic granule exocytosis are often not found, again suggesting that this model is incomplete.

The TLRs also have been implicated in cytokine storm syndromes. For instance, TLR4 is known to be important for cytokine release secondary to gram-negative bacterial sepsis (9). MAS is most closely associated with systemic juvenile idiopathic arthritis (SJIA), a disorder that has been recently associated with abnormal TLR-induced gene expression patterns (10). Though these gene expression changes cannot be linked to a particular TLR, this observation suggests a possible role for TLR activation in MAS as well. However, since in MAS gram-negative organisms are not found and since primary HLH is often initiated by viral infections that do not trigger TLR4, it is likely there are other TLRs that drive the inflammatory syndrome in the these entities.

Our understanding of the immunopathology of HLH/MAS is limited by the availability of animal models. Those that exist require infectious agents to trigger disease, which makes it difficult to separate the infectious pathology from the immunopathology of the cytokine storm itself. Therefore, we undertook a series of studies to determine whether repeated TLR stimulation, without exogenous antigen, could replicate an MAS-like syndrome. A previous report identified systemic toxicity with repeated TLR9 stimulation with CpG DNA (11). CpG DNA is a potent stimulator of TLR9 (12). In agreement with the report by Heikenwalder et al. of systemic toxicity (11), we found that mice treated with repeated TLR9 agonism developed cytopenia, splenomegaly, hep-

Conflict of interest: The authors have declared that no conflict of interest exists.
Citation for this article: *J Clin Invest.* 2011;121(6):2264–2277. doi:10.1172/JCI43157.

atitis, microthrombosis, and hyperferritinemia, consistent with MAS-like syndromes (13). As in the infectious HLH model, we show that CpG cytokine storm syndrome was IFN-γ dependent but resulted in only minimal $CD8^+$ T cell activation. Surprisingly, the syndrome was not dependent on B or T cells, implying that TLR9 activation of innate immune cells is sufficient to initiate the disease. We also show that NK cells were dispensable for disease. However, deleting both T/B cells and NK cells simultaneously resulted in disease attenuation, suggesting that the disease is at least partially dependent on the presence of both populations together. We further show that DCs were capable of IFN-γ transcription after CpG treatment and that deletion of conventional DCs (cDCs) resulted in a partial reduction of circulating IFN-γ in response to CpG administration. We also identified IL-10 as a negative regulator of the MAS-like pathology. Mice made hyporesponsive to IL-10 developed a more severe phenotype, including the presence of large amounts of hemophagocytosis, a pathologic finding not seen when IL-10 signaling is intact. Based on these findings, we propose what we believe to be a new model for the MAS-like cytokine storm syndromes, in which overstimulation of innate immunity by TLRs rather than adaptive immunity is sufficient for disease development and in which the spectrum of disease severity is in part controlled by responsiveness to IL-10.

Results

Repeated TLR stimulation leads to the clinical appearance of the cytokine storm syndrome. We examined whether repeated TLR agonism could reproduce elements of the MAS cytokine storm syndrome in the absence of exogenous antigen. Repeated administration of the TLR9 agonist CpG to mice resulted in a peripheral pancytopenia (Figure 1A, rbc indices shown in Supplemental Figure 1; supplemental material available online with this article; doi:10.1172/JCI43157DS1). While absolute numbers of granulocytes were slightly fewer in CpG-treated mice, the majority of the leukopenia was accounted for by a reduction in lymphocyte numbers (Figure 1B). CpG-treated mice also developed a marked splenomegaly (Figure 1C). This increase in splenic size was accompanied by an increase in cellularity (Figure 1D). However, the absolute numbers of lymphocytes, macrophages, and DCs did not change dramatically in the spleen (data not shown), suggesting that the peripheral lymphopenia is not due simply to splenic sequestration. Similar results were also obtained with repeated TLR3 or TLR4 agonism (data not shown), albeit to a lesser extent.

As in the MAS syndrome, CpG-treated mice developed elevated serum ferritin (Figure 1E) after 10 days of treatment. Patients with MAS also develop a disseminated intravascular coagulopathy (DIC) (14–17), usually assessed by decreased serum fibrinogen. Interestingly, mice treated repeatedly with CpG (herein referred to as "repeated CpG-treated mice") did not show any decrease in fibrinogen compared with that in PBS controls (data not shown). Since fibrinogen levels were only modestly decreased in the perforin-deficient murine model of primary HLH (8), and since it was not assessed in either the Rab27a-deficient (18) or Munc-13-4–deficient models (19), it remained possible that plasma fibrinogen was not a sensitive assay of the DIC pathophysiologic state. We therefore looked for the histologic correlate of DIC, the presence of microthrombi on tissue sections. Three out of six livers from CpG-treated mice developed thrombi in their small vessels, with lobular necrosis adjacent to these vessels (Figure 1F). None of the PBS-treated mice developed thrombi or necrosis. Even in the CpG-treated mice without thrombosis, all of the livers showed evidence of vascular damage, including endothelial cell plumpness, endothelial cell lifting, and inflammatory infiltrate. These lesions may be precursors to the thrombi noted in 50% of the CpG-treated livers examined. Notably, none of these changes were seen in PBS-treated mice. These data are suggestive of an incompletely penetrant DIC state present in CpG-treated mice.

To test whether multiple CpG injections were required, we examined mice injected with a single dose of CpG. Mice given 1 injection of CpG, followed by 4 PBS injections, displayed completely normal blood counts, ferritin levels, spleen size, and liver and spleen histology (data not shown). Mice examined 24 hours after a single injection of CpG did not have anemia, splenomegaly, hyperferritinemia, or hepatic or splenic histologic changes but did develop a leukopenia and thrombocytopenia (Supplemental Figure 1 and data not shown). Thus, it appears that multiple doses of CpG are required to induce the complete disease of pancytopenia, splenomegaly, hyperferritinemia, microthrombosis, and hepatitis. Because it has been suggested that CpG motifs may trigger other receptors besides TLR9 (20), we attempted to induce disease in TLR9-deficient (*Tlr9*$^{-/-}$) mice but found that CpG-treated *Tlr9*$^{-/-}$ mice were indistinguishable from mice injected with PBS (Supplemental Figure 2 and data not shown), thus demonstrating that this CpG-induced disease is mediated through TLR9 stimulation.

Repeated TLR9 stimulation results in the development of other MAS-associated pathology. HLH/MAS is associated with an increase in Th1 cytokines, particularly serum IFN-γ. Mice treated with multiple doses of CpG also demonstrate elevated serum IFN-γ at sacrifice on day 10 after initial CpG treatment (Figure 2A). We also assessed IL-12p70, IL-6, and IL-10 levels in the serum and found them to be elevated (Figure 2A). Increased levels of all of these cytokines are found in HLH/MAS in both murine models and in human patients (18, 21). The amount of IFN-γ produced in this model is not as high as that seen in primary HLH, both in humans and mice, and may reflect the less severe phenotype seen in the repeated CpG-treated mice. In contrast, we did not find significant amounts of serum TNF-α (data not shown). HLH/MAS is often associated with hepatitis, and CpG-treated mice developed both lobular and portal inflammation in all of the livers examined (Figure 2, B–D). We next characterized the type of cellular infiltrate by immunohistochemistry. Livers from CpG-treated mice showed a lymphohistiocytic infiltrate consisting predominately of macrophages and to a lesser degree a mixture of T and B cells (Figure 2E). Splenic architecture was disrupted, with a loss of B cell areas and an infiltration of the red pulp by a large number of small nucleated cells (Figure 2F), consistent with other reports of spleens from CpG-treated mice (11). Consistent with reports of bone marrow pathology in primary HLH murine models (18), the bone marrow of CpG-treated mice showed decreased cellularity but increased megakaryocyte numbers (Supplemental Figure 3). In summary, repeated TLR9 activation, even in the absence of foreign antigen, can recapitulate multiple serologic and histologic features of the MAS cytokine storm syndrome.

IFN-γ is required for maximal disease expression in repeated CpG-treated mice. IFN-γ is the central cytokine mediating primary HLH syndromes, and neutralization of this antibody ameliorates disease (8, 22). We therefore tested the hypothesis that the TLR9-induced MAS-like syndrome would also be IFN-γ dependent. *Ifng*$^{-/-}$ mice were treated with repeated CpG injections, as described above. Compared with wild-type counterparts, *Ifng*$^{-/-}$ mice did not develop

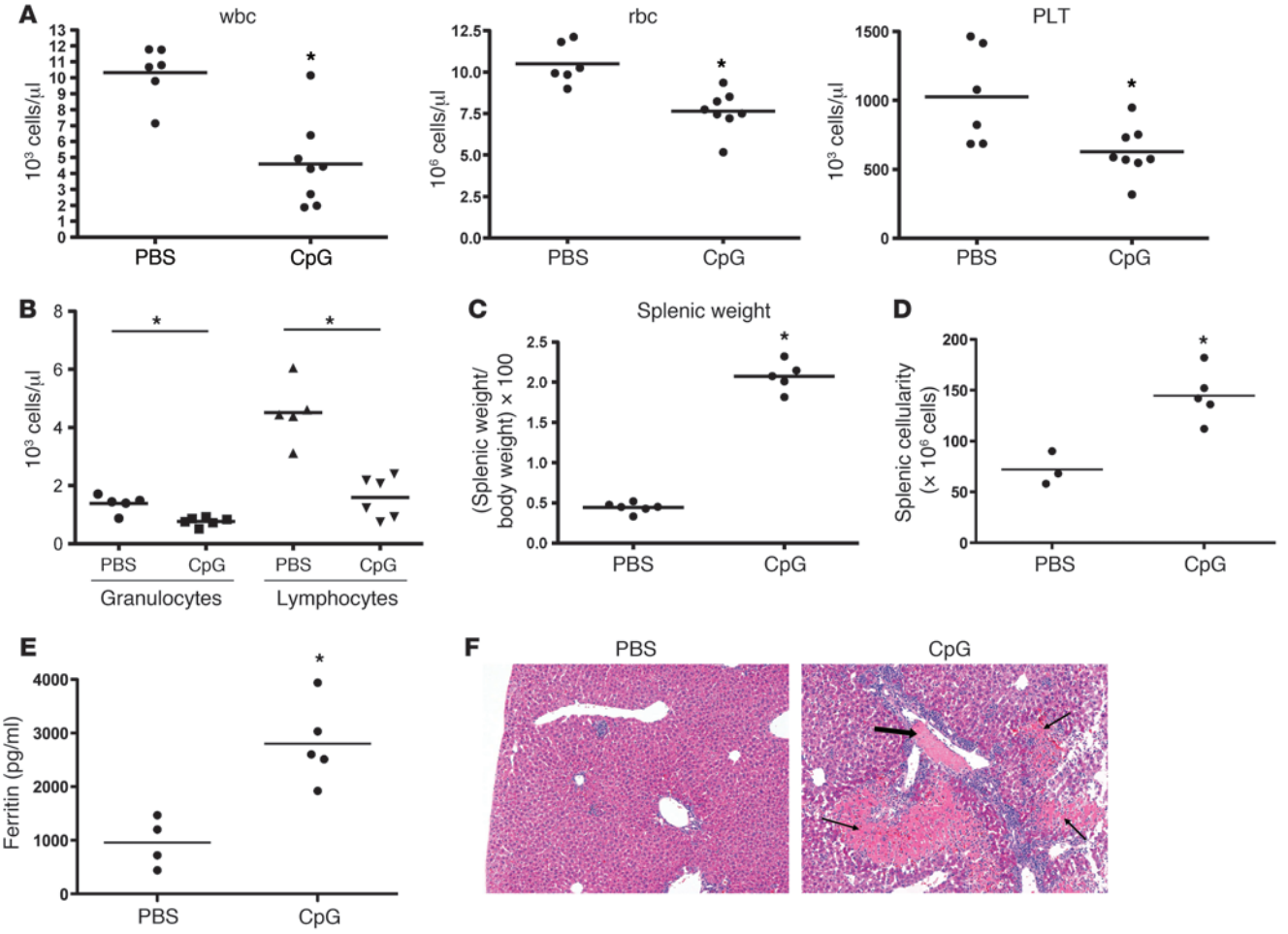

Figure 1

Repeatedly CpG-treated mice develop clinical features of cytokine storm. Mice were treated over a 10-day period with repeated injections of PBS or CpG (50 μg) every 2 days. (**A**) Blood was sampled on day 8 for a complete blood count and analyzed for total leukocytes (wbc), rbc, and platelets (PLT). (**B**) The leukopenia associated with CpG treatment was further characterized by assessing lymphocyte and granulocyte numbers. (**C**–**E**) Analyses were performed at sacrifice on day 10. (**C** and **D**) Spleens from mice were weighed and are expressed at a ratio to total body weight. Total splenocyte numbers were assessed by counts with a hemacytometer. (**E**) Serum ferritin was measured by ELISA. (**F**) Livers from mice were sectioned and stained with H&E (original magnification, ×40). Fibrin thrombi (thick arrows) and associated tissue necrosis (thin arrows) were seen only in CpG-treated mice. Individual symbols each represent 1 mouse, with the horizontal lines representing the mean values. *$P < 0.05$ versus PBS for all panels. Data are representative of 3 experiments.

anemia or thrombocytopenia (Figure 3, A and B), had markedly reduced splenomegaly (Figure 3C), did not develop hepatic inflammation (Figure 3D), and manifested preservation of splenic architecture (data not shown). However, not all elements of the CpG-mediated MAS-like syndrome were IFN-γ dependent, in particular, the leukopenia (Figure 3A) and hyperferritinemia (Figure 3E). Because the amounts of IFN-γ produced at day 10 of disease were much lower than what is seen in lymphocytic choriomeningitis virus models of HLH (ref. 8 and Figure 2A), we further characterized the kinetics of IFN-γ produced earlier in the course of disease. Mice were administered repeated CpG injections for 3 doses, and IFN-γ was measured 18 hours after each dose. We found that there was an initial burst of IFN-γ produced after the first administration of CpG, which then fell nearly to baseline levels. This was followed by a plateau of low level IFN-γ after the third injection (day 6), comparable to what was seen at day 10 (Figure 2A and Figure 4A). Thus, there appear to be 2 phases of IFN-γ production, an initial high burst followed by a plateau of lower amounts of IFN-γ.

To test whether only the high burst of IFN-γ was required for CpG-induced cytokine storm, we administered an IFN-γ–neutralizing antibody either before or after the mice experienced the initial peak of IFN-γ. Mice were treated with CpG over 10 days, as described above, with IFN-γ neutralization initiated at day 0 or at day 3 (Figure 4, B and C). Mice that received IFN-γ neutralization throughout the entire experiment phenocopied the *Ifng*$^{-/-}$ mice, confirming that IFN-γ production is critical for development of disease. Mice that did not receive IFN-γ neutralization until day 3, allowing them to experience only the initial burst of IFN-γ but not the long tail of IFN-γ activity (second-phase blockade), also failed to develop disease. This observation demonstrates that although the amount of IFN-γ seen at the later time points is modest, it is crucial to the development of pathology. These experiments con-

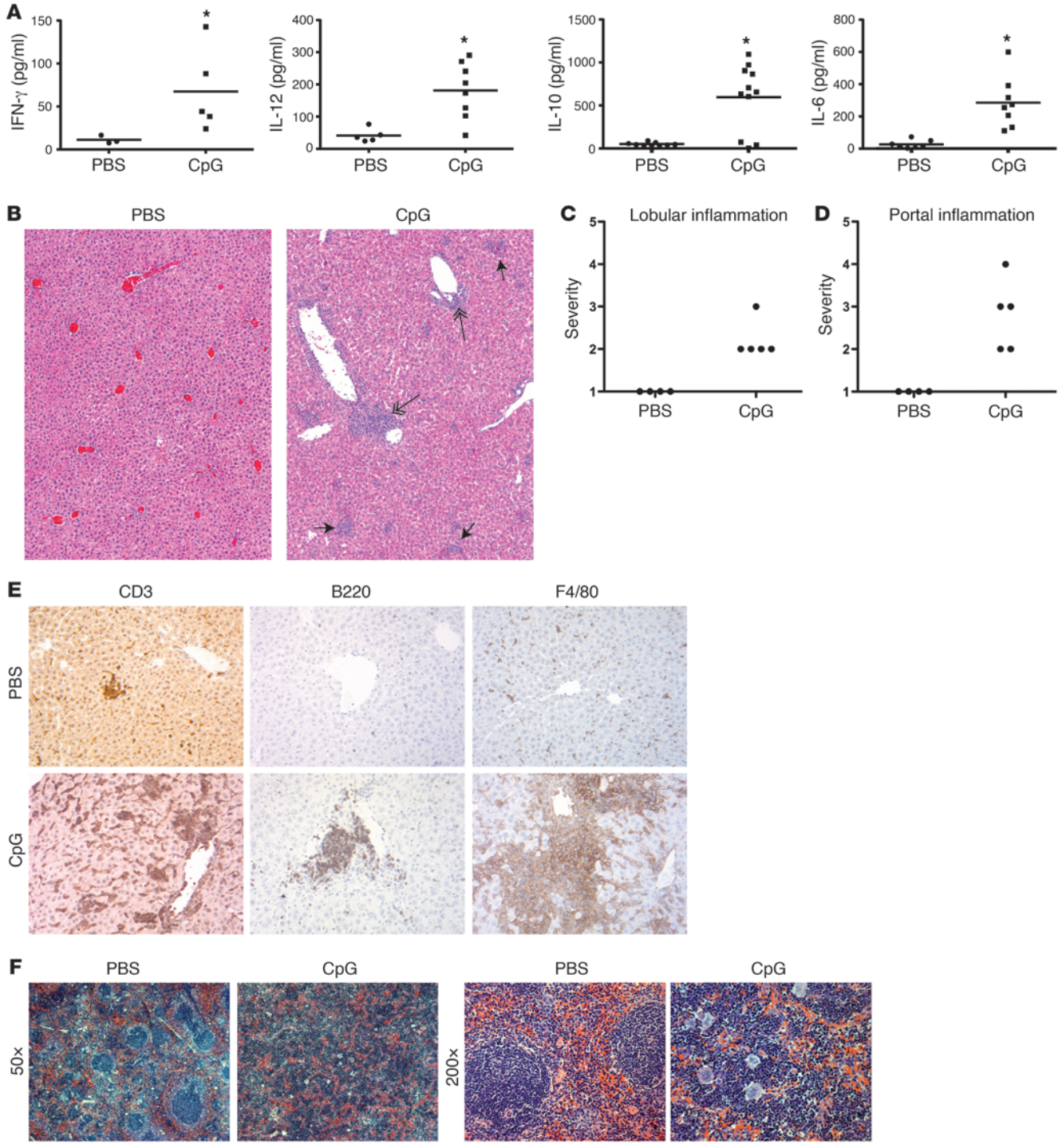

Figure 2

Repeatedly CpG-treated mice develop serologic and histologic features of cytokine storm. Mice were treated with PBS and CpG as in Figure 1. (**A**) Serum levels of IFN-γ, IL-12, IL-10, and IL-6 were assessed by ELISA at day 10. (**B**–**D**) Hepatic inflammation was assessed at sacrifice on day 10 by a blinded pathologist using a standardized scoring system as follows: portal inflammation, 0, absent; 1, focal and minimal; 2, mild; 3, moderate; 4, marked; lobular inflammation, 0, absent; 1, rare small foci; 2, occasional small foci; 3, moderate small foci; 4, frequent small foci. (**B**) Livers were stained with H&E. Lobular infiltrates are marked with short arrows, and portal infiltrates are marked with long double arrows. Representative sections are shown at an original magnification of ×40. (**C**) Lobular and (**D**) portal inflammation were scored separately. (**E**) Hepatic infiltrates were stained by immunohistochemistry for T cell (CD3), B cell (B220), and macrophage (F4/80) markers. Representative sections are shown at an original magnification of ×200. (**F**) Splenic architecture was assessed by H&E stains of spleens on day 10 (original magnification, ×50 [left]; ×200 [right]). *$P < 0.05$ versus PBS for all experiments. Data are representative of 3 experiments. Individual symbols each represent 1 mouse, with the horizontal lines representing the mean values.

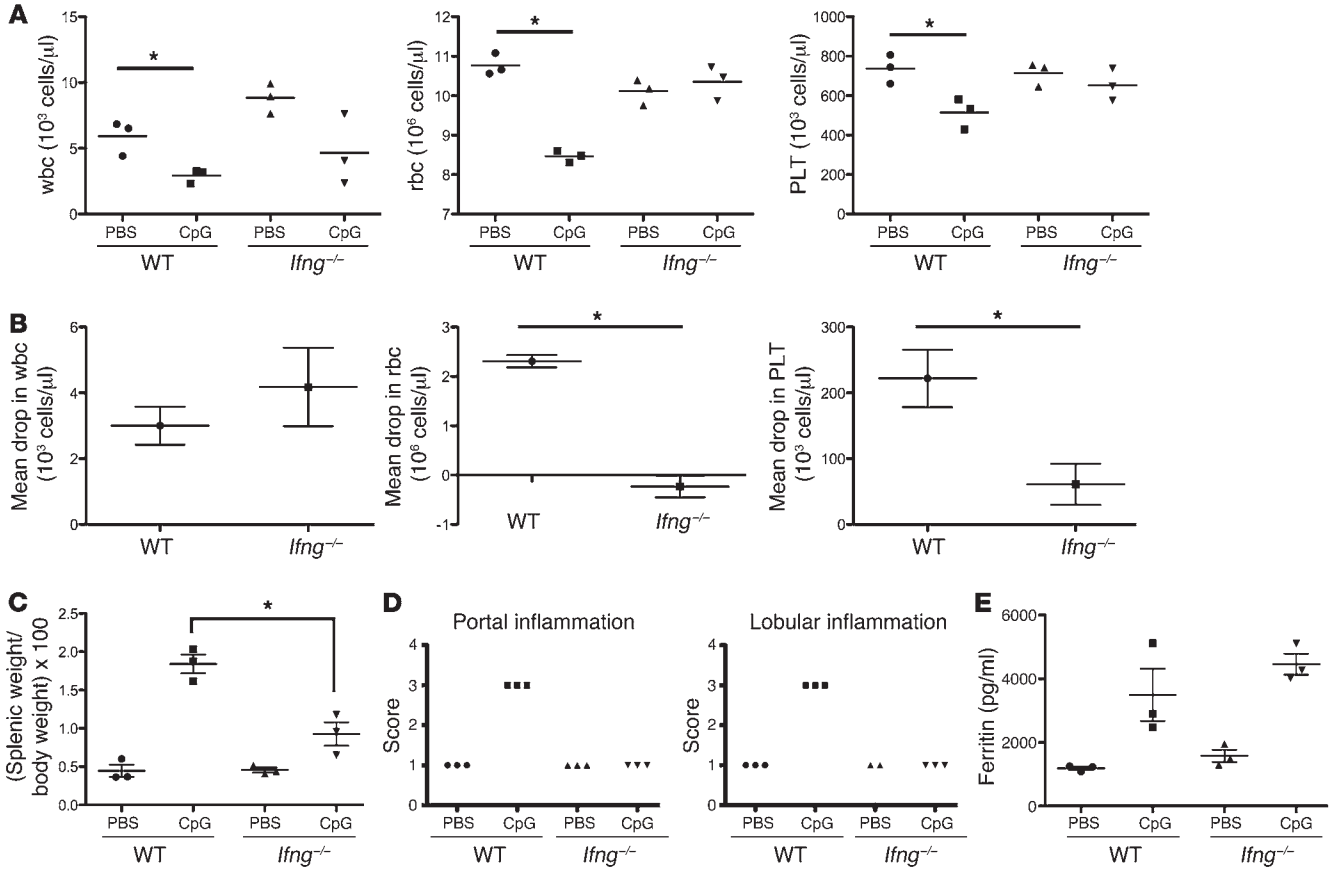

Figure 3

IFN-γ is required for maximal CpG-induced cytokine storm disease expression. *Ifng*$^{-/-}$ mice were treated with PBS or CpG, and data are analyzed as in Figure 1. Compared with wild-type counterparts, (**A** and **B**) *Ifng*$^{-/-}$ mice have reduced anemia and thrombocytopenia, (**C**) reduced splenomegaly, and (**D**) complete elimination of hepatic inflammation. In contrast to the experiments shown in Figure 1, there was no difference in (**A** and **B**) the degree of leukopenia or (**E**) hyperferritinemia. *$P < 0.05$. Data are representative of 3 experiments. Individual symbols each represent 1 mouse, with the horizontal lines representing the mean values.

firm the central role of IFN-γ in CpG-mediated cytokine storm syndrome and its similarity to MAS-like syndromes.

Although we did not find significant amounts of TNF-α present in the sera of CpG-treated mice, there remained a possibility that TNF-α was being produced at time points we were not measuring and contributing to disease pathogenesis. To exclude this possibility, we also treated mice with TNF-α–neutralizing antibody every 3 days during the 10-day course of repeated CpG treatments. TNF-α–neutralized mice did not show any decrease in any disease parameters compared with mice receiving isotype control antibody (data not shown), suggesting that TNF-α is not necessary for the development of the MAS-like syndrome.

Repeated TLR9-stimulated mice do not develop excess hemophagocytosis. An expansion of hemophagocytosing macrophages is typically found in the cytokine storm syndromes (5, 13, 23, 24). It is unclear whether these cells are causal or reactive in the process. Both mice and humans exhibit low levels of continuous hemophagocytosis, and hemophagocytosing cells were detected in the bone marrow and spleen of normal mice (Supplemental Figure 3), representing on average 1 hemophagocyte per longitudinal section of femur or cross section of spleen. After repeated CpG stimulation, we did not find an increase in the numbers of hemophagocytes in the bone marrow, spleen, or liver. This observation was consistent with negative immunohistochemical staining for CD163, a marker expressed on the surface of hemophagocytosing macrophages, in both the marrow and spleen (Supplemental Figure 3 and data not shown). To ensure that our protocols are appropriate for the identification of these cells, we examined the marrows of perforin-deficient mice infected with lymphocytic choriomeningitis virus and found more than 15 hemophagocytes per high-powered field (Supplemental Figure 3 and data not shown), arguing against the possibility that our detection methods were insufficient to detect hemophagocytosis. These data suggest that robust hemophagocytosis is not required for the development of other clinical abnormalities associated with MAS initiated by repeated TLR9 stimulation.

CpG-initiated MAS is accompanied by only minimal CD8$^+$ T cell activation. Because of the known role of CD8$^+$ T cells in the development of primary HLH, we expected to see robust activation of this population in CpG-induced MAS syndrome. Surprisingly, we found only minimal activation. A very small but consistent increase in the number of CD69$^+$CD62L^{lo}CD8$^+$ T cells was seen in CpG-treated mice (Supplemental Figure 4, A and B). No increase in the number of CD69$^+$CD62L^{lo}CD4$^+$ T cells or B cells was seen, suggesting that this activation was specific to CD8$^+$ T cells. Next,

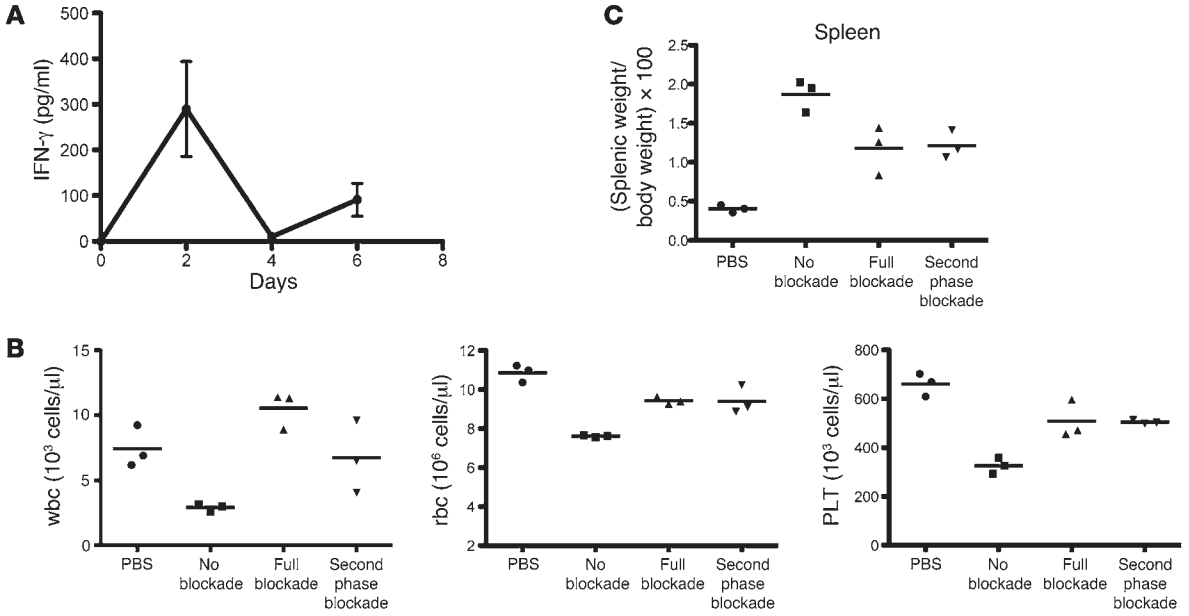

Figure 4
Blockade of late-phase IFN-γ is sufficient to ameliorate disease. (**A**) Levels of IFN-γ were measured from mice repeatedly injected with CpG, showing a biphasic response with an early higher level followed by lower levels, comparable to what is seen on day 10 (Figure 2A). (**B** and **C**) Mice were treated with PBS alone (PBS) or repeated CpG injections along with an IFN-γ–neutralizing antibody from day 0 (full blockade) or day 3 (second-phase blockade) or with an irrelevant isotype antibody (no blockade). (**B**) Cell counts were measured at sacrifice on day 10. (**C**) Spleen size (ratio of splenic weight to total body weight) was assessed at sacrifice. Data are representative of 2 experiments. Individual symbols each represent 1 mouse, with the horizontal lines representing the mean values.

we examined whether repeated CpG treatment primed $CD8^+$ T cells to make IFN-γ. Splenocytes were isolated from repeated CpG- or PBS-treated mice and incubated for 5 hours with BFA, PMA, and ionomycin. $CD8^+$ T cells but not $CD4^+$ T cells showed a small subpopulation of high IFN-γ–producing cells found only in the spleens of mice treated with CpG (Supplemental Figure 4C). These data show that only a small population of $CD8^+$ T cells acquire activation markers and produce IFN-γ, suggesting that these cells are not likely to be contributing greatly to the CpG-induced pathology.

$CD8^+$ T cells are not required for CpG-mediated MAS-like syndrome. Given that current models of HLH/MAS pathophysiology are centered on $CD8^+$ T cell activation, we were surprised that the extent of $CD8^+$ T cell activation was low in CpG-mediated MAS. This finding suggested the possibility that although some $CD8^+$ T cells are activated, they are not the only effector cells in this model. Therefore, we tested whether the CpG-mediated pathology occurs in mice lacking $CD8^+$ T cells by treating β_2 microglobulin–deficient (*$B2m^{-/-}$*) mice with repeated CpG injections. *$B2m^{-/-}$* mice lack both $CD8^+$ T cells (25) and NKT cells (26), due to the absence of MHC I and CD1d molecules, respectively. We found no difference in the cytopenia or splenomegaly of CpG-treated *$B2m^{-/-}$* mice compared with those of wild-type controls (Figure 5, A and B). Additionally, we detected no differences in the hepatic inflammation, presence of thrombi and necrosis, or in serum ferritin levels (data not shown). These results show that neither $CD8^+$ T cells nor NKT cells are required for CpG-mediated MAS. In fact, we found that *$B2m^{-/-}$* mice consistently produced more IFN-γ than wild-type mice, suggesting that the absence of $CD8^+$ and NKT cells enhances the repeated TLR9-stimulated phenotype (data not shown).

Adaptive immunity is not required for CpG-induced MAS-like syndrome. Given the surprising result that $CD8^+$ T cells were not required for CpG-induced disease, we next investigated whether adaptive immunity was required at all. We tested this requirement by attempting to induce disease in recombination activating gene 2–deficient (*$Rag2^{-/-}$*) mice, which lack T cells, B cells, and NKT cells, using the same CpG protocol described above. *$Rag2^{-/-}$* mice developed anemia, thrombocytopenia, splenomegaly, and hyperferritinemia, similar to wild-type controls, and had an enhanced liver microthrombosis and hepatitis (Figure 5, C–F). *$Rag2^{-/-}$* mice display leukopenia at baseline, due to their lack of lymphocytes. This leukopenia is not worsened with CpG treatment (Figure 5C), as would be expected given our data that granulocytes are largely unaffected by the CpG treatment (Figure 1B). CpG-treated *$Rag2^{-/-}$* mice had an elevated serum IFN-γ, similar to that of wild-type mice, demonstrating that non-lymphocyte cells are sufficient to produce CpG-induced IFN-γ.

NK cells are activated in repeated CpG-treated mice. We next considered other known IFN-γ–producing effector cells that might be mediating disease. Given that $CD4^+$ T cells appeared relatively unaffected by CpG (Supplemental Figure 4), we investigated the contribution of NK cells to this process. NK cell numbers showed a greater than 20-fold decrease in the spleens of mice that received repeated CpG treatment (Figure 6A), suggesting either that they were activated and exiting the spleen or that they were being consumed in the process of disease progression. To examine whether splenic NK cells were activated by CpG treatment, we evaluated light scatter profile, CD69 upregulation, and IFN-γ production 16 hours after a single injection of CpG. CD69 was upregulated, and there was a dramatic increase in both forward and side scatter of splenic NK cells in mice treated with CpG. However, IFN-γ was

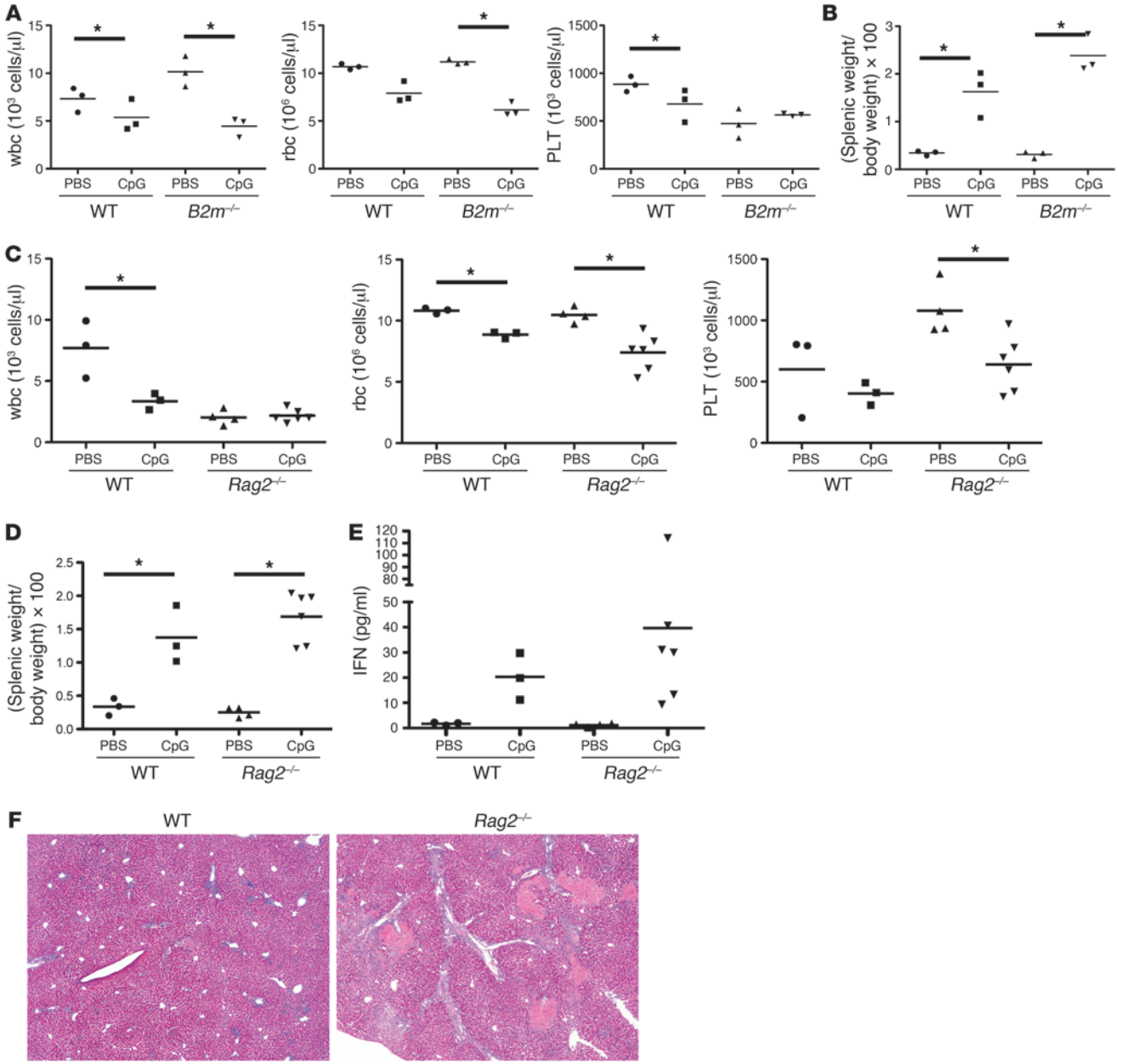

Figure 5

Adaptive immunity is not required for CpG-induced cytopenia or splenomegaly or IFN production. (**A** and **B**) Wild-type or *B2m*$^{-/-}$ mice were treated with PBS or CpG as in Figure 1. (**A**) Peripheral blood cell counts were measured at 8 days and (**B**) spleen size measured at sacrifice at day 10. Results are representative of 2 experiments. (**C**–**E**) WT and *Rag2*$^{-/-}$ mice were treated with PBS or CpG as in Figure 1. (**C**) Peripheral blood cell counts were assessed at day 8, and (**D**) spleen size was assessed at sacrifice at day 10. (**E**) IFN levels in the blood were assessed by serum ELISA (day 10) for each group of mice. Data are representative of 2 experiments. (**F**) Liver sections taken at day sacrifice on day were stained by H&E. Representative sections are shown at an original magnification of ×40. Individual symbols each represent 1 mouse, with the horizontal lines representing the mean values. *$P < 0.05$ versus PBS for all panels.

not dramatically increased in NK cells at this time. The increase in CD69 expression in NK cells was also seen in *B2m*$^{-/-}$ mice, suggesting that this NK cell activation did not require the presence of CD8$^+$ T cells (Figure 6B).

A combination of NK cells and lymphocytes is required for maximal disease expression in CpG-induced MAS-like syndrome. We next investigated whether NK cells were necessary to cause CpG-induced disease by depleting this lineage with the anti-NK1.1 antibody, PK136. Mice repeatedly treated with PK136 and CpG were devoid of NK cells in the peripheral blood and liver (Supplemental Figure 5A). It is impossible to assess depletion from spleen, since the repeated CpG treatment itself causes complete NK depletion from this site (Figure 6A). NK cell–depleted mice developed cytopenia, splenomegaly, hyperferritinemia, hepatitis, and elevated IFN-γ lev-

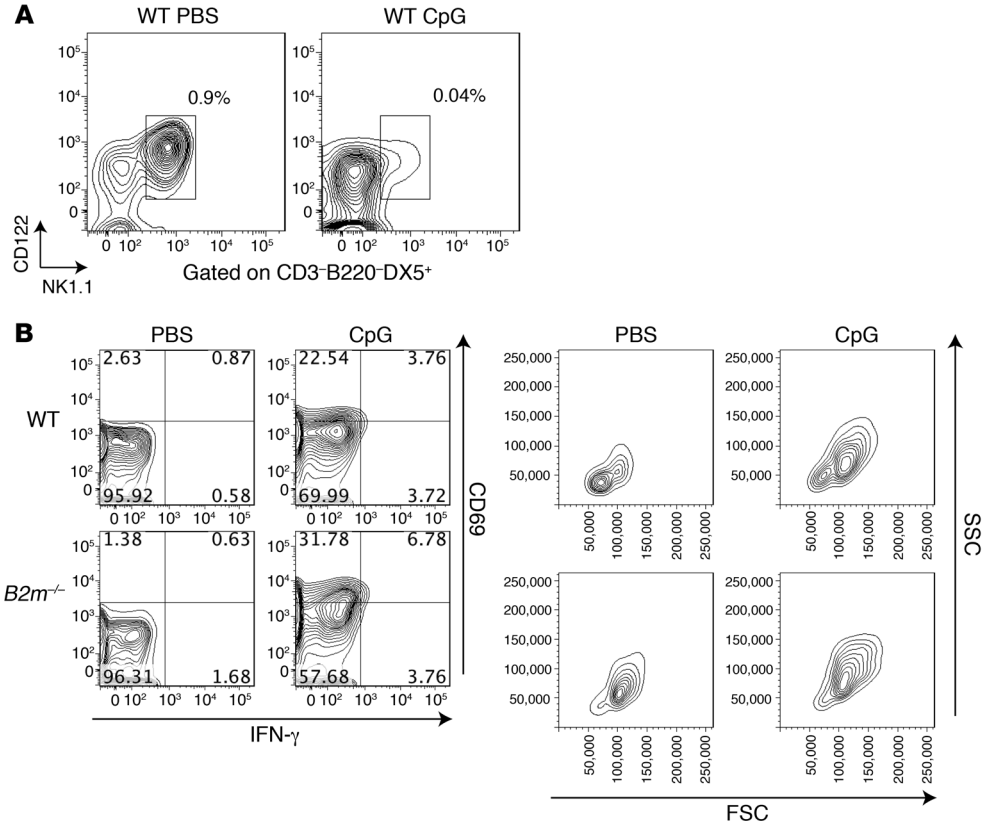

Figure 6
NK cells are activated by CpG treatment. Wild-type mice were treated with CpG as in Figure 1. (**A**) NK cells, identified as CD3⁻B220⁻NK1.1⁺CD122⁺DX5⁺ cells, are virtually absent in the spleens of wild-type mice treated with CpG. Percentages shown are of total splenic lymphocytes. Plots are representative of 3 experiments. (**B**) Splenic NK cells from wild-type and *B2m*$^{-/-}$ mice were analyzed for CD69, IFN-γ, and light scatter changes 16 hours after a single CpG injection. The numbers represent the percentage of NK cells falling into each quadrant of the CD69/IFN-γ plot. Plots are representative of 3 experiments. Data are representative of 3 experiments. FSC, forward scatter; SSC, side scatter.

els similar to isotype antibody-treated controls (Supplemental Figure 5, B and C, and data not shown), suggesting that NK cells were dispensable. Given that both *Rag2*$^{-/-}$ mice and NK cell–depleted mice both develop disease, we hypothesized that either NK cells or T cells could compensate for the absence of one another. To examine this possibility, we treated mice doubly deficient for Rag2 and the cytokine receptor common γ-chain (*Rag2*$^{-/-}$*Il2rg*$^{-/-}$) with CpG. These mice lack all lymphocyte populations, including T cells and NK cells. *Rag2*$^{-/-}$*Il2rg*$^{-/-}$ mice treated with repeated CpG injection showed attenuation in many but not all disease parameters. There was a marked preservation of peripheral blood counts and a decrease in splenomegaly compared with those of *Rag2*$^{-/-}$ mice (Figure 7A). However, the degree of hepatitis was unchanged (Figure 7B). Consistent with a partial rescue from the IFN-γ–dependent aspects of the model, *Rag2*$^{-/-}$*Il2rg*$^{-/-}$ CpG-treated mice demonstrated an approximate 50% reduction in the levels of IFN-γ measured on day 10 of disease (Figure 7C). These results suggest that although a combination of NK cells and T/B cells are required for maximal disease expression and IFN-γ production, another non-lymphocyte population plays an important role in CpG-induced MAS.

The IFN-γ–producing cellular compartment changes from the first phase to the second phase of TLR9-induced MAS-like syndrome. To examine IFN-γ production by nonlymphoid cell populations, we made use of the Yeti IFN-γ reporter mouse. This mouse reports active IFN-γ transcription by marking these cells with yellow florescent protein (YFP) (27). A caveat to these mice is that translation may be independent of transcription of IFN-γ and that some cell populations may be transcribing IFN-γ at baseline and, therefore, YFP^{+} at rest (27). Nonetheless, these mice allowed us to examine IFN-γ production in cellular populations that are otherwise difficult to assess. We first examined control mice treated with PBS. In all PBS-treated mice tested, we noted subpopulations of plasmacytoid DCs (pDCs) and CD8α^{+} cDCs in the liver that showed IFN-γ transcription as marked by YFP positivity, suggesting that these cells are transcribing IFN-γ message at baseline (Supplemental Figure 6). Next, we examined both spleens and livers after a single injection (early phase) and after 4 injections (late phase) of CpG. In mice that received 1 dose of CpG (i.e., the early phase of IFN-γ production), there was a small but consistent increase in YFP intensity in liver CD8α^{+} cDCs and pDCs, consistent with an increase in IFN-γ transcription. After 4 injections of CpG (i.e., late-phase IFN-γ production), splenic pDCs showed a dramatic increase in the numbers of IFN-γ–transcribing cells, demonstrating a shift in IFN-γ–producing populations between the 2 phases of the disease (Supplemental Figure 6). Thus, both CD8α^{+} cDCs and pDCs are likely contributing to the production of IFN-γ in our repeated CpG treatment model, again suggesting a nonlymphoid-derived IFN-γ source. Most lymphocyte populations showed variable YFP positivity between mice; however, NKT cells also consistently showed increased YFP positivity in the late phase, again providing a cellular correlate to the biphasic IFN-γ serum response (data not shown).

CD11c^{+} cDCs are required for the initial IFN-γ surge but not for second-phase IFN-γ production or disease. Since CD11c^{+} DCs were implicated in IFN-γ production and since ablation of all lymphocyte populations still resulted in substantial disease (Figure 7, A and B), we next tested whether ablation of DCs could ameliorate disease. We made use of the CD11c-DTR mouse (28), which deletes CD11c^{+} cDCs upon diphtheria toxin (DT) administration. It is important to note that pDCs are relatively spared in this model (29). Because

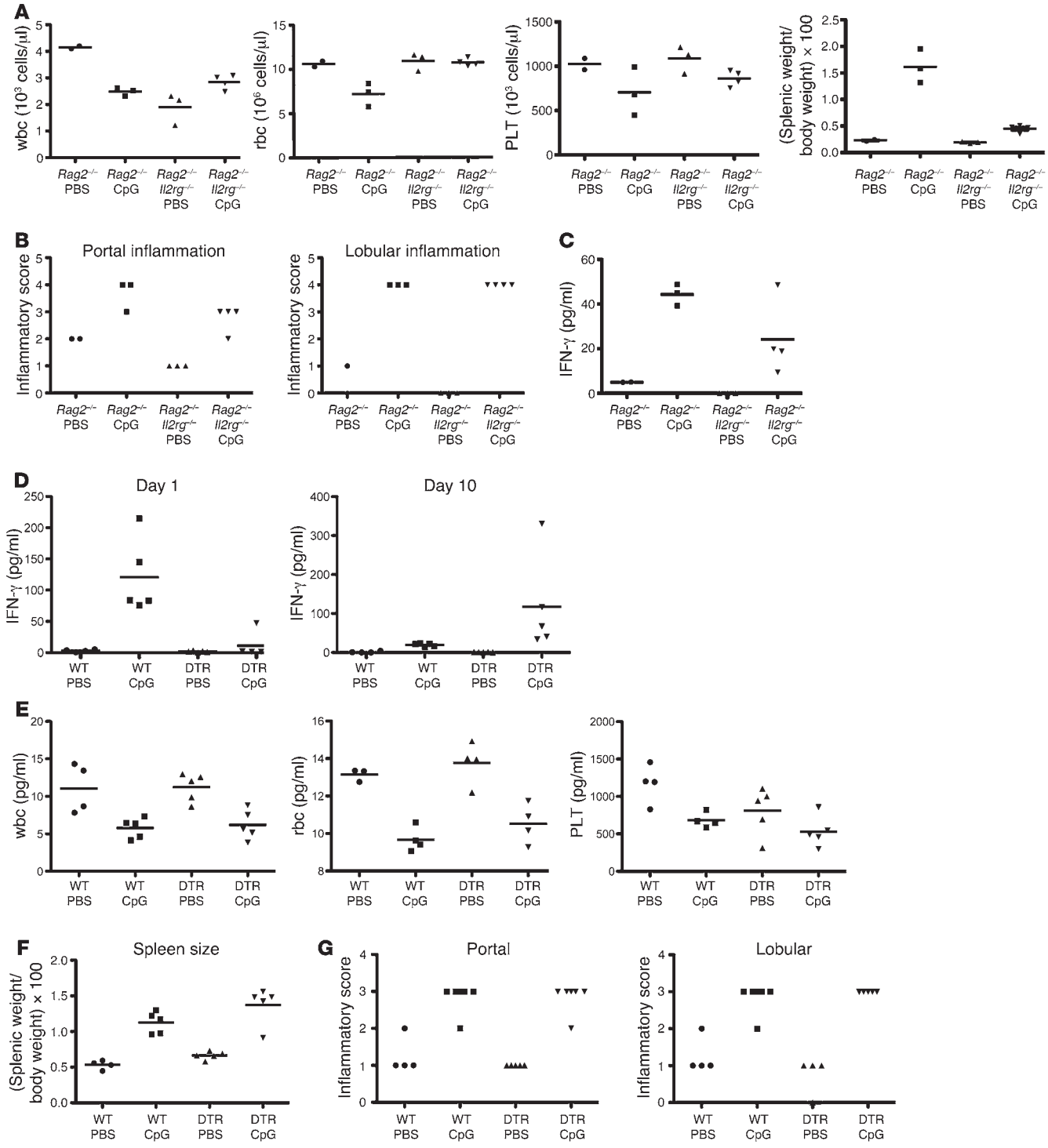

Figure 7

Simultaneous deletion of NK cells and lymphocytes partially reduces the severity of CpG-induced HLH/MAS-like syndrome, whereas cDCs are required for early-phase IFN-γ production but are dispensable for disease. (**A**–**C**) *Rag2*$^{-/-}$ and *Rag2*$^{-/-}$*Il2rg*$^{-/-}$ mice were treated with repeated PBS or CpG injections as in Figure 1. (**A**) Peripheral blood counts were assessed at day 8, and spleen size was assessed at day 10. (**B**) Liver inflammation, assessed at day 10, was quantitated as in Figure 2. (**C**) Serum IFN-γ levels were also assessed at day 10. Data are representative of 2 experiments. (**D**–**G**) CD11c-DTR marrow was injected into lethally irradiated wild-type mice that were then allowed to rest for 8 weeks. These mice were then injected on alternating days with DT (100 ng) and either CpG or PBS as in Figure 1. (**D**) IFN-γ levels were measured by ELISA on day 1 and day 10. (**E**) Peripheral blood counts were assessed at day 8, and (**F**) spleen size was assessed at day 10. (**G**) Liver inflammation, assessed at day 10, was quantitated as in Figure 2. Individual symbols each represent 1 mouse, with the horizontal lines representing the mean values.

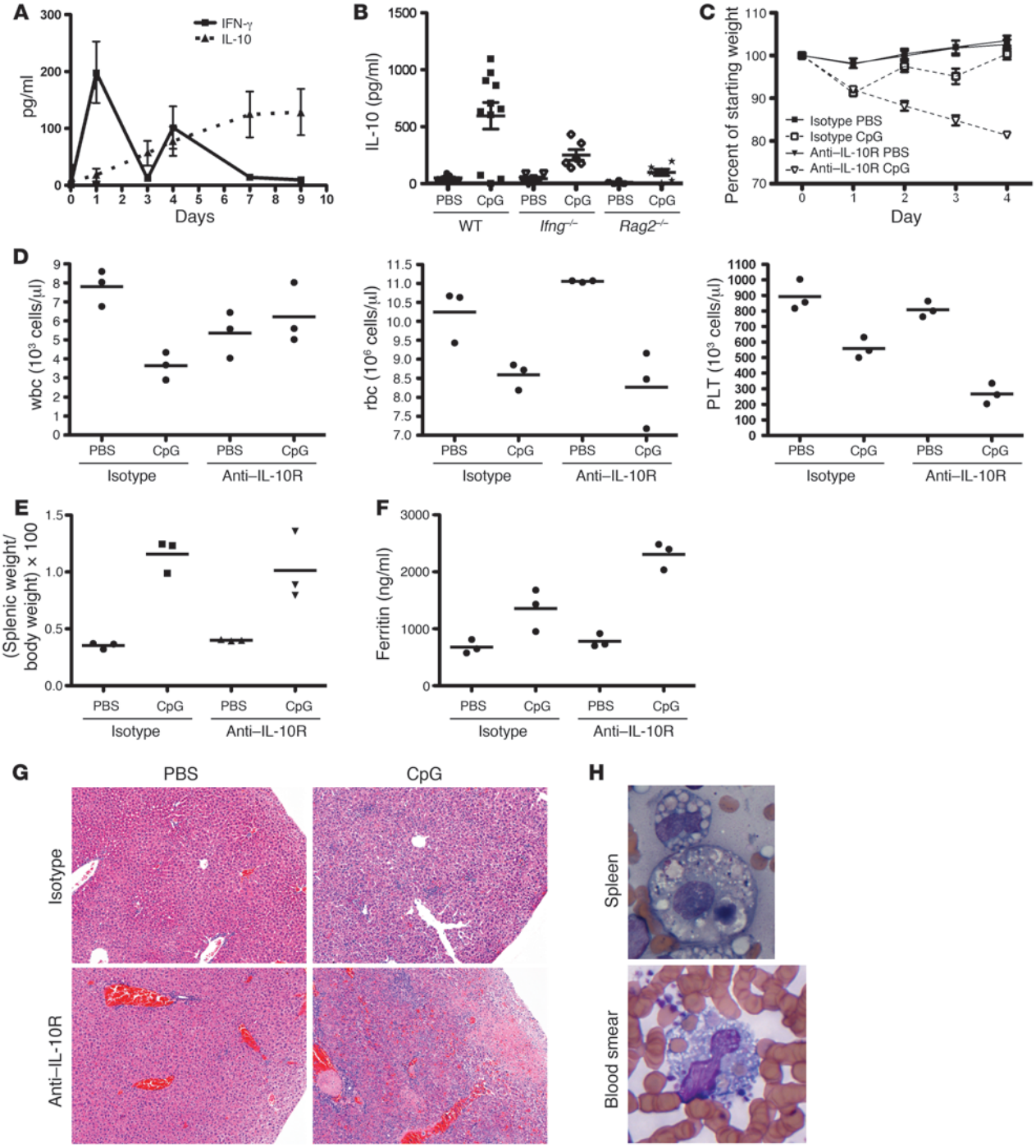

Figure 8

IL-10 receptor blockade results in a more severe MAS-like phenotype with the presence of hemophagocytosis. (**A**) Serum IL-10 (dotted line) and IFN-γ (solid line) levels were measured by ELISA over the course of repeated CpG injections. (**B**) Serum IL-10 levels were measured by ELISA at day 10 of repeated CpG injection in wild-type, *Ifng*$^{-/-}$, and *Rag2*$^{-/-}$ mice. (**C**–**F**) Mice were given repeated CpG or PBS injections according to the same schedule as in Figure 1. Mice were given concurrent injections of isotype or anti–IL-10R antibody with each dose. (**C**) Daily weights were measured, (**D**) complete blood count was performed on day 5, and (**E**) splenic weight and (**F**) serum ferritin were measured at sacrifice at day 6, when most mice receiving anti–IL-10R treatment became moribund. (**G**) Livers taken at sacrifice on day 6 were stained by H&E. Representative sections are shown at an original magnification of ×100. (**H**) Splenic touch preparations were made at sacrifice on day 6, and peripheral blood smears made at the time of complete blood count on day 5 were stained by Wright-Giemsa and evaluated for hemophagocytosis. Representative fields (original magnification, ×1,000 fields) are shown for mice receiving both CpG and anti–IL-10R antibody. All results are representative of 3–4 experiments. Individual symbols each represent 1 mouse, with the horizontal lines representing the mean values.

repeated DT administration is lethal to a CD11c-DTR mouse, we made bone marrow chimeras using wild-type or CD11c-DTR donors into wild-type animals. This approach allowed us to maintain excellent depletion of $CD11c^+$ DCs over the course of the 10-day experiment (Supplemental Figure 7). cDC-depleted mice produced essentially no IFN-γ after the initial CpG injection; however, these mice were able to make IFN-γ at day 10 (Figure 7D). These mice also developed cytopenia, splenomegaly, and hepatitis comparable with DC-sufficient controls (Figure 7, E–G). Thus, although cDCs are required for the initial IFN-γ spike, they appear dispensable for later-phase IFN-γ and disease expression. This cDC requirement could be due to direct production by cDCs, as suggested by the IFN-γ reporter experiments, or by cDC interaction with other cell types such as lymphocytes. These data are consistent with our finding that the second phase of lower level IFN-γ production was required for disease initiation (Figure 4, B and C) as well as the fact that pDCs, which are not deleted in the CD11c-DTR system, increased their IFN-γ production in the second phase (Supplemental Figure 6).

IL-10 plays a protective role in TLR9-induced MAS-like syndrome and limits the development of hemophagocytosis. Primary HLH resulting from genetic deficiencies in cytotoxic granule exocytosis is usually very severe in its phenotype both in humans and in mice. However, the secondary form of MAS can be quite varied, ranging from the subclinical to the severe. Our model of TLR9 induced MAS-like syndrome is on the mild end of this spectrum. In considering the mild severity of the phenotype, we observed that the mice were producing significant IL-10 in response to CpG (Figure 2A). IL-10 is well recognized to be an antiinflammatory cytokine, and we considered whether CpG-induced IL-10 may be contributing mild phenotype of our model. In order to better define the kinetics of IL-10 production, we measured IL-10 and IFN-γ throughout the course of repeated injections (Figure 8A). We again observed a biphasic IFN-γ response over time. In contrast, IL-10 levels rose monotonically over the course of injections. We next tested whether the rising IL-10 levels were in response to production of IFN-γ by examining IL-10 levels in the serum of *Ifng*$^{-/-}$ mice treated with repeated CpG injections (Figure 8B). Interestingly, *Ifng*$^{-/-}$ mice made much less IL-10 compared with that of control mice, suggesting that IL-10 was indeed being made in response to *Ifng*$^{-/-}$. We also examined IL-10 levels in *Rag2*$^{-/-}$ mice to test whether lymphocytes are responsible for IL-10 production. Although, as noted above, these mice made as much IFN-γ as their wild-type counterparts (Figure 5E), IL-10 levels were quite reduced (Figure 8B), suggesting a role for lymphocytes in CpG-induced IL-10. The correlation of the decreased IL-10 levels in *Rag2*$^{-/-}$ mice with the increased hepatic pathology (Figure 5F) further suggested that IL-10 was acting to suppress disease activity.

In order to directly test the role of IL-10 in this model, we performed repeated injections of CpG, concurrent with repeated injections of IL-10 receptor blocking antibody (anti–IL-10R, clone 1B1.3A). Mice that received repeated anti–IL-10R with PBS injections showed no phenotype; however, mice that received both anti–IL-10R and CpG treatments became severely ill, uniformly becoming moribund between days 6–8 of the experiment. Treatment of mice with anti–IL-10R with CpG resulted in severe weight loss, increased thrombocytopenia, and increased hyperferritinemia compared with those that received isotype antibody (Figure 8, C–F). Interestingly, not all components of the disease were enhanced, as leukopenia, anemia, and splenomegaly were not increased. Liver disease was dramatically worse with anti–IL-10R treatment, with large areas of necrosis, increased microthrombi, and large areas of inflammatory infiltrate (Figure 8G). These findings were similar to the liver pathology seen in the *Rag2*$^{-/-}$ mice (Figure 5E). Most strikingly, mice treated with anti–IL-10R and CpG developed large amounts of hemophagocytosis, easily seen in both splenic touch preparations and in peripheral blood smears (Figure 8H). Hemophagocytosis was also identified on touch preparations made from livers taken at sacrifice, demonstrating the presence of hemophagocytes infiltrating the liver as well (data not shown). Thus, repeated TLR9 stimulation, concurrent with blockade of IL-10 receptor, results in an MAS-like syndrome that represents the severe end of the spectrum, including the presence of hemophagocytes, suggesting that IL-10 levels can modulate the severity of the disease.

Discussion

Cytokine storm syndrome can result from inflammation from bacterial infection, ineffective clearance of virus, rheumatologic disease, or, in many instances, from an unknown source. In each of these cases, it is possible that this inflammation may arise from antigen-specific responses of either B cells or T cells or from non-antigen-specific inflammation from pattern recognition receptors, particularly the TLRs. Because of the role of IFN-γ and the requirement for $CD8^+$ T cells in murine models of primary HLH (8), there has been much attention given to the antigen-specific receptors in cytokine storm. In this report, we show that an MAS-like cytokine storm syndrome can be driven by TLR9 in an IFN-γ–dependent manner but does not require exogenous antigen or adaptive immunity. Although some of the consequences of repeated CpG administration had been reported earlier (11), we now recognize the syndrome as an MAS-like cytokine storm and extend these results to mechanistic cytokines and effector cell compartments. Both our own data with other TLR ligands and previous reports (11) suggest that TLR9 agonism is unique in producing this MAS-like syndrome. The severity of MAS in this model is less than that seen in the perforin-deficient model (8). However, multiple groups have suggested that as opposed to primary HLH, which is often severe and life threatening, MAS consists of a spectrum of disease severity (10, 30). The more mild phenotype of our model allows us to perform an immunologic dissection of the pathophysiology, without confounding effects from severe morbidity and early mortality. Interestingly, this mild phenotype is a result of the anti-inflammatory activity of IL-10. This IL-10 is produced partly in response to the TLR9-induced IFN-γ, since CpG-treated mice deficient in IFN-γ make less IL-10 than wild-type mice. Blocking IL-10 results in an enhanced phenotype, more similar in its course to primary HLH and fulminant MAS, with rapid onset of death and large amounts of hemophagocytes. It is conceivable that differing IL-10 responses contribute to the variability of severity of MAS in human disease as well, since IL-10 is a cytokine that has been documented to be elevated in human patients (21). Intriguingly, an IL-10–responsive gene signature was one of the most prominent patterns of gene expression found in a recent study of peripheral blood mononuclear cells from primary HLH patients (31).

The data presented in this report support the idea that hyperactive innate immune responses, such as those associated with SJIA, can lead to IFN-γ production and the MAS phenotype. It is interesting to speculate whether the same process might also play some role in primary familial HLH, in which antigen-driven $CD8^+$ T cells are clearly the major disease-inducing compartment (8).

While viral antigens are not eliminated in primary HLH, there is also ineffective clearance of viral nucleic acid. These nucleic acids can serve as a source for continuous TLR stimulation, causing an "adjuvantemia" in addition to persistent antigenemia. Future studies will be directed at testing this hypothesis.

The most commonly implicated virus in the development of HLH in humans is EBV, a DNA virus that triggers TLR9 (32). Patients with EBV-HLH have much higher viral loads compared with patients with EBV infectious mononucleosis without HLH (33). This increased viral load might serve as a source of TLR9 stimulus in these patients, leading to some of the pathologic findings. MAS is recognized also as a complication of systemic lupus erythematosus (34), a disease that has been linked to TLR9 overstimulation by self DNA (35–38). Patients with SJIA, another population at risk for MAS, show gene expression profiles consistent with repeated TLR/IL-1 receptor activation (10). What drives this response is unclear. One hypothesis suggests an intrinsic hyperactivity of TLR/IL-1 receptor signaling, perhaps in the absence of extrinsic adjuvant. This "pseduo-adjuvantemia" might be in part what drives the progression to MAS in these patients. In fact, we and others have reported that upon closer inspection, one-third of SJIA patients show mild signs of MAS, 3-times greater than the previously recognized 10% (30, 39). This observation argues that MAS immunopathology plays a more central role in the disease process of SJIA, as might be predicted by our model of repeated TLR-induced MAS and the data on the gene signatures of TLR activation in these patients. Our results suggest TLR blockade, such as with antagonist CpGs, as a potential novel therapeutic avenue for all of these cytokine storm conditions.

Our model also revealed that disease develops in the absence of hemophagocytes, a cell type often found in cytokine storm syndromes, whose role remains unclear. It has been proposed that hemophagocytes are inhibitors of inflammatory responses, as $CD163^+$ macrophages produce antiinflammatory cytokines such as IL-10 (40). Hemophagocytes are also a source of heme-oxygenase 1, another mediator of antiinflammatory responses (41). In contrast, others have suggested that the ingestion and destruction of hematopoietic cells might be part of the pathologic process of MAS, particularly with respect to the cytopenias (42, 43). Although sampling error is always of concern, it has been reported that over 40% of patients with MAS/HLH do not have hemophagocytes in bone marrow aspirates, suggesting a separation of disease initiation from the development of hemophagocytes (23). Given that we see pancytopenia in the absence of abundant hemophagocytosis, it is difficult to argue for a role for these cells in the development of these low cells counts. We also see many other elements of the disease, despite the lack of hemophagocytes. The disease severity in our model is milder than fulminate primary HLH, raising 2 possibilities for the absence of hemophagocytes: first, these cells do mediate HLH/MAS toxicity, and in their absence, a more mild course is seen, or second, these cell are indeed reactive and antiinflammatory and are therefore not induced in a milder form of the disease. When IL-10R is blocked, a more severe disease results, along with the presence of large amounts hemophagocytosis. This result makes a correlation of hemophagocytosis with more severe disease; however, the direction of the causality remains undetermined. Future experiments will need to be performed to determine whether hemophagocytes cause enhanced disease or appear in reaction against more severe disease.

While IFN-γ is clearly an important effector cytokine in TLR9-mediated cytokine storm, we were unable to identify a single IFN-γ–producing population that was required for disease. $CD8^+$ T cells, NK cells, and NKT cells were not required for the induction of disease. However, when B cells, T cells, and NK cells were removed together, a marked reduction in disease severity was seen, suggesting that NK cells and lymphocytes together are critical for maximal disease. Interestingly, there continued to be production of IFN-γ, albeit at a lower lever, and concomitant liver disease in *Rag2*$^{-/-}$*Il2rg*$^{-/-}$ mice. This observation is consistent with our finding that both cDCs and pDCs are transcribing IFN-γ in our model. The critical IFN-γ–producing cell also changes with time, as evidenced by the CD11c-DTR experiments, demonstrating the importance of the cDC in early IFN-γ production but not the later phase. It is also possible that other tissues besides the spleen and liver may be harboring pathogenic IFN-γ–producing cells. Future studies will address these issues. It is also of interest to note that the inflammatory cells seen in the livers of the *Rag2*$^{-/-}$ and the *Rag2*$^{-/-}$*Il2rg*$^{-/-}$ CpG-treated mice must be innate immune cells. Although in an animal with a complete immune system, the hepatic infiltrate is predominately lymphocytic, in the absence of adaptive immunity, we see that the innate immune system can also cause pathogenic inflammation in the MAS disease process.

TLR agonists are increasingly being used in vaccination strategies as a means of enhancing the response to specific antigen (44). CpG DNA in particular has been proposed as an adjuvant for enhancing vaccines. It is reassuring that a single dose of CpG was not sufficient to induce the MAS-like disease. However, our results suggest caution in multiple-dose vaccination strategies using CpG. Further investigation will be needed to determine whether repeated doses spaced further apart in time might not lead to the onset of the MAS-like syndrome and how repeated coadministration with antigen might change the response.

Herein we have reported what we believe to be a new model of MAS-like cytokine storm that uses TLR9 stimulation. We propose that TLR activation, in the case of high viral load in EBV-HLH, self DNA/RNA in SLE, or intrinsic hyperactivity in SJIA, may lead to the cytokine storm syndrome. Our results also provide a possible explanation for the spectrum of severity of secondary MAS, in that IL-10 responsiveness can change the degree of pathology seen, including the presence of hemophagocytosis. Differences in IL-10 responsiveness could be due to host factors in polymorphisms of IL-10 or IL-10 receptor signaling machinery or in polymorphisms in viral IL-10 produced by MAS inducing viruses such as EBV (45).

Furthermore, this study suggests that TLR or IFN-γ blockade might be useful therapeutic avenues to explore in the appropriate clinical setting. Importantly, the disease process can be ameliorated by IFN-γ blockade, even if given after the initial inflammatory stimulus. Mice treated with neutralizing antibody at day 3 had a reduction of symptoms of the same magnitude as that of mice treated before disease induction. This finding raises the possibility that IFN-γ–neutralizing antibody may be of therapeutic benefit, even in patients early in their disease course. The role of IL-10 in suppressing disease activity makes this cytokine another exciting target for possible therapeutic intervention.

Methods

Antibodies and reagents. CD3, CD4, CD8, CD19, CD62L, CD69, and IFN-γ fluorochrome-tagged antibodies were all purchased from BD Pharmingen. For intracellular staining with IFN-γ, we used the BD Pharmingen Intracellular Staining Kit according to the manufacturer's instructions. CpG 1826 oligonucleotide was synthesized by IDT. XMG1.2 (anti–IFN-γ), XT3.11 (anti–TNF-α), PK136 (anti-NK1.1), 1B1.3A (anti–IL-10R), and

HRPN (isotype control) were purchased from Bio-X-Cell. PK136 was used at a dose 0.1 mg per injection daily throughout depletion experiments, starting the day before the first injection. XMG1.2 was used at a dose of 0.5 mg for the first 2 doses and then 0.15 mg per dose thereafter. XMG1.2 was given concurrently with CpG injection at the time points described in Results. XT3.11 was used at a dose of 1.5 mg i.p. every 3 days. 1B1.3A was given concurrently with CpG injections at a dose of 0.2 mg i.p.

Mice. C57BL/6, *B2m*$^{-/-}$, *Rag2*$^{-/-}$, CD11c-DTR, and *Ifng*$^{-/-}$ mice were purchased from The Jackson Laboratory and housed in our Association for Assessment and Accreditation of Laboratory Animal Care–certified animal facility. *Rag2*$^{-/-}$*Il2rg*$^{-/-}$ mice were purchased from Taconic Laboratories (46). Yeti mice were a gift from M. Mohrs (Trudeau Institute, Saranac Lake, New York, USA) (27). All experiments were performed with approval of the University of Pennsylvania and The Children's Hospital of Philadelphia IACUC. Mice were injected i.p. on days 0, 2, 4, 7, and 9 with PBS, CpG (50 μg), LPS (100 μg), or polyinosinic/polycytidylic acid (50 μg) in 200 μl of volume. On day 8, peripheral blood was sampled by cheek bleed, and a complete blood count was performed on a Hemavet analyzer. On day 10, mice were euthanized, and organs and serum were taken for analysis.

DC depletion experiments. In order to generate mice capable of long-term DC depletion, C57BL/6 mice were exposed to 10.5 gray of gamma irradiation, followed by i.v. injection of 1 million bone marrow cells from either C57BL/6 mice or CD11c-DTR mice. These mice were allowed to recover for 8 weeks before use in an experiment. Mice were treated with 100 ng DT (Sigma-Aldrich) on day –1 and then every other day during the course of an experiment.

ELISA. IFN-γ, IL-12, IL-10, and IL-6 ELISA kits were purchased from BD Pharmingen and used according to the manufacturer's instructions. Ferritin ELISA was purchased from ALPCO and used according to the manufacturer's instructions.

Histology. Unperfused organ sections were fixed overnight in 4% paraformaldehyde and embedded in paraffin. Liver and spleen sections were stained with H&E and were read by a pediatric pathologist blinded to treatment protocols. Aspirates of marrow were taken from femurs and made into dry smears on glass slides. These were stained with Wright-Giemsa. Bones were decalcified for 1 week before sectioning and H&E staining to analyze the marrow. All marrow and spleen slides were scored by a hematopathologist blinded to the treatment protocol. CD163, CD3, B220, and F4/80 immunohistochemistry was performed on slides after antigen retrieval with a pressure cooker. Detection was performed using the Mouse-on-Mouse (M.O.M.) Basic, Vectastain ABC (rabbit), or Vectastain ABC (rat) Kits where appropriate (Vector Laboratories), followed by DAB reagent (Dako). Hemophagocytosis was identified on H&E- and Wright-Giemsa–stained slides by morphologic inspection by a board-certified pediatric hematopathologist. CD163 staining was used to confirm hemophagocytosis.

Statistics. Data were plotted and analyzed using Prism 5.0 (GraphPad Software). Statistical significance was tested for using 2-tailed Student's *t* test or the Mann-Whitney test, as appropriate, with $P < 0.05$ set as a cutoff for significance. Error bars in all figures represent SEM, with the midline representing the mean value.

Acknowledgments

The authors would like to thank Kim Nichols and Tao Zou for their critical review of this manuscript. E.M. Behrens was supported by an Arthritis Foundation Innovative Research Grant, the Howard Hughes Medical Institute Early Career Physician Scientist Award, and an NIH/NIAID grant (K08AI079396).

Received for publication July 22, 2010, and accepted in revised form April 4, 2011.

Address correspondence to: Edward M. Behrens, 1107C ARC, 3615 Civic Center Blvd., Philadelphia, Pennsylvania 19104, USA. Phone: 267.426.0142; Fax: 215.590.1258; E-mail: behrens@email.chop.edu.

1. Suntharalingam G, et al. Cytokine storm in a phase 1 trial of the anti-CD28 monoclonal antibody TGN1412. *N Engl J Med*. 2006;355(10):1018–1028.
2. Sriskandan S, Altmann DM. The immunology of sepsis. *J Pathol*. 2008;214(2):211–223.
3. Fujiwara F, Hibi S, Imashuku S. Hypercytokinemia in hemophagocytic syndrome. *Am J Pediatr Hematol Oncol*. 1993;15(1):92–98.
4. Amaral MC, Alves JD. Pathogenesis of multi-organic failure in autoimmune diseases. *Autoimmun Rev*. 2009;8(6):525–528.
5. Castillo L, Carcillo J. Secondary hemophagocytic lymphohistiocytosis and severe sepsis/ systemic inflammatory response syndrome/multiorgan dysfunction syndrome/macrophage activation syndrome share common intermediate phenotypes on a spectrum of inflammation. *Pediatr Crit Care Med*. 2009; 10(3):387–392.
6. Tracey KJ, et al. Shock and tissue injury induced by recombinant human cachectin. *Science*. 1986; 234(4775):470–474.
7. Tang Y, et al. Early diagnostic and prognostic significance of a specific Th1/Th2 cytokine pattern in children with haemophagocytic syndrome. *Br J Haematol*. 2008;143(1):84–91.
8. Jordan MB, Hildeman D, Kappler J, Marrack P. An animal model of hemophagocytic lymphohistiocytosis (HLH): CD8+ T cells and interferon gamma are essential for the disorder. *Blood*. 2004; 104(3):735–743.
9. Poltorak A, et al. Defective LPS signaling in C3H/HeJ and C57BL/10ScCr mice: mutations in Tlr4 gene. *Science*. 1998;282(5396):2085–2088.
10. Fall N, et al. Gene expression profiling of peripheral blood from patients with untreated new-onset systemic juvenile idiopathic arthritis reveals molecular heterogeneity that may predict macrophage activation syndrome. *Arthritis Rheum*. 2007;56(11):3793–3804.
11. Heikenwalder M, et al. Lymphoid follicle destruction and immunosuppression after repeated CpG oligodeoxynucleotide administration. *Nat Med*. 2004; 10(2):187–192.
12. Krieg AM, et al. CpG motifs in bacterial DNA trigger direct B-cell activation. *Nature*. 1995; 374(6522):546–549.
13. Henter JI, et al. HLH-2004: Diagnostic and therapeutic guidelines for hemophagocytic lymphohistiocytosis. *Pediatr Blood Cancer*. 2007;48(2):124–131.
14. De Vere-Tyndall A, Macauley D, Ansell BM. Disseminated intravascular coagulation complicating systemic juvenile chronic arthritis ("Still's disease"). *Clin Rheumatol*. 1983;2(4):415–418.
15. Scott JP, Gerber P, Maryjowski MC, Pachman LM. Evidence for intravascular coagulation in systemic onset, but not polyarticular, juvenile rheumatoid arthritis. *Arthritis Rheum*. 1985;28(3):256–261.
16. Silverman ED, Miller JJ 3rd, Bernstein B, Shafai T. Consumption coagulopathy associated with systemic juvenile rheumatoid arthritis. *J Pediatr*. 1983; 103(6):872–876.
17. Wong KF, Chan JK. Reactive hemophagocytic syndrome--a clinicopathologic study of 40 patients in an Oriental population. *Am J Med*. 1992;93(2):177–180.
18. Pachlopnik Schmid J, et al. A Griscelli syndrome type 2 murine model of hemophagocytic lymphohistiocytosis (HLH). *Eur J Immunol*. 2008;38(11):3219–3225.
19. Crozat K, et al. Jinx, an MCMV susceptibility phenotype caused by disruption of Unc13d: a mouse model of type 3 familial hemophagocytic lymphohistiocytosis. *J Exp Med*. 2007;204(4):853–863.
20. Sanjuan MA, et al. CpG-induced tyrosine phosphorylation occurs via a TLR9-independent mechanism and is required for cytokine secretion. *J Cell Biol*. 2006;172(7):1057–1068.
21. Osugi Y, et al. Cytokine production regulating Th1 and Th2 cytokines in hemophagocytic lymphohistiocytosis. *Blood*. 1997;89(11):4100–4103.
22. Pachlopnik Schmid J, et al. Neutralization of IFNgamma defeats haemophagocytosis in LCMV-infected perforin- and Rab27a-deficient mice. *EMBO Mol Med*. 2009;1(2):112–124.
23. Gupta A, Tyrrell P, Valani R, Benseler S, Weitzman S, Abdelhaleem M. The role of the initial bone marrow aspirate in the diagnosis of hemophagocytic lymphohistiocytosis. *Pediatr Blood Cancer*. 2008; 51(3):402–404.
24. Hara T, et al. Histiocytic hemophagocytosis in the bone marrow in children with sepsis and disseminated intravascular coagulation. *Acta Paediatr Jpn*. 1989;31(3):335–339.
25. Koller BH, Marrack P, Kappler JW, Smithies O. Normal development of mice deficient in beta 2M, MHC class I proteins, and CD8+ T cells. *Science*. 1990; 248(4960):1227–1230.
26. Coles MC, Raulet DH. Class I dependence of the development of CD4+ CD8- NK1.1+ thymocytes. *J Exp Med*. 1994;180(1):395–399.
27. Stetson DB, et al. Constitutive cytokine mRNAs mark natural killer (NK) and NK T cells poised for rapid effector function. *J Exp Med*. 2003;198(7):1069–1076.
28. Caton ML, Smith-Raska MR, Reizis B. Notch-RBP-J signaling controls the homeostasis of CD8- dendritic cells in the spleen. *J Exp Med*. 2007;204(7):1653–1664.
29. Bennett CL, Clausen BE. DC ablation in mice: promises, pitfalls, and challenges. *Trends Immunol*.

2007;28(12):525–531.
30. Behrens EM, Beukelman T, Paessler M, Cron RQ. Occult macrophage activation syndrome in patients with systemic juvenile idiopathic arthritis. *J Rheumatol*. 2007;34(5):1133–1138.
31. Sumegi J, et al. Gene expression profiling of peripheral blood mononuclear cells from children with active hemophagocytic lymphohistiocytosis [published online ahead of print February 16, 2011]. *Blood*. doi:10.1182/blood-2010-08-300046.
32. Guggemoos S, Hangel D, Hamm S, Heit A, Bauer S, Adler H. TLR9 contributes to antiviral immunity during gammaherpesvirus infection. *J Immunol*. 2008; 180(1):438–443.
33. Teramura T, Tabata Y, Yagi T, Morimoto A, Hibi S, Imashuku S. Quantitative analysis of cell-free Epstein-Barr virus genome copy number in patients with EBV-associated hemophagocytic lymphohistiocytosis. *Leuk Lymphoma*. 2002;43(1):173–179.
34. Parodi A, et al. Macrophage activation syndrome in juvenile systemic lupus erythematosus: a multinational multicenter study of thirty-eight patients. *Arthritis Rheum*. 2009;60(11):3388–3399.
35. Avalos AM, Busconi L, Marshak-Rothstein A. Regulation of autoreactive B cell responses to endogenous TLR ligands. *Autoimmunity*. 2009;43(1):76–83.
36. Christensen SR, Shupe J, Nickerson K, Kashgarian M, Flavell RA, Shlomchik MJ. Toll-like receptor 7 and TLR9 dictate autoantibody specificity and have opposing inflammatory and regulatory roles in a murine model of lupus. *Immunity*. 2006;25(3):417–428.
37. Lartigue A, et al. Role of TLR9 in anti-nucleosome and anti-DNA antibody production in lpr mutation-induced murine lupus. *J Immunol*. 2006; 177(2):1349–1354.
38. Xu CJ, Zhang WH, Pan HF, Li XP, Xu JH, Ye DQ. Association study of a single nucleotide polymorphism in the exon 2 region of toll-like receptor 9 (TLR9) gene with susceptibility to systemic lupus erythematosus among Chinese. *Mol Biol Rep*. 2009; 36(8):2245–2248.
39. Bleesing J, et al. The diagnostic significance of soluble CD163 and soluble interleukin-2 receptor alpha-chain in macrophage activation syndrome and untreated new-onset systemic juvenile idiopathic arthritis. *Arthritis Rheum*. 2007;56(3):965–971.
40. Verreck FA, de Boer T, Langenberg DM, van der Zanden L, Ottenhoff TH. Phenotypic and functional profiling of human proinflammatory type-1 and anti-inflammatory type-2 macrophages in response to microbial antigens and IFN-gamma- and CD40L-mediated costimulation. *J Leukoc Biol*. 2006; 79(2):285–293.
41. Schaer CA, Schoedon G, Imhof A, Kurrer MO, Schaer DJ. Constitutive endocytosis of CD163 mediates hemoglobin-heme uptake and determines the noninflammatory and protective transcriptional response of macrophages to hemoglobin. *Circ Res*. 2006;99(9):943–950.
42. Francois B, Trimoreau F, Vignon P, Fixe P, Praloran V, Gastinne H. Thrombocytopenia in the sepsis syndrome: role of hemophagocytosis and macrophage colony-stimulating factor. *Am J Med*. 1997; 103(2):114–120.
43. Yarali N, Balaban I, Akyurek N, Ucar S, Zorlu P. Hemophagocytosis: the cause of anemia and thrombocytopenia in congenital syphilis. *Pediatr Hematol Oncol*. 2009;26(6):461–466.
44. Lahiri A, Das P, Chakravortty D. Engagement of TLR signaling as adjuvant: towards smarter vaccine and beyond. *Vaccine*. 2008;26(52):6777–6783.
45. Kanai K, et al. The vIL-10 gene of the Epstein-Barr virus (EBV) is conserved in a stable manner except for a few point mutations in various EBV isolates. *Virus Genes*. 2007;35(3):563–569.
46. Cao X, et al. Defective lymphoid development in mice lacking expression of the common cytokine receptor gamma chain. *Immunity*. 1995;2(3):223–238.